Dani et al. 2024. *Int. J. Vehicle Structures & Systems*, 16(4), 630-635
ISSN: 0975-3060 (Print), 0975-3540 (Online)
doi: 10.4273/ijvss.16.4.24

International Journal of Vehicle Structures & Systems
Available online at https://yanthrika.com/eja

Optimizing the Properties of AA 5052 Alloys through Silicon Carbide and Groundnut Shell Ash Reinforcements

M.S. Heaven Dani[a], N. Saravanan[b], L. Girisha[c], K. Kiran Uday[d], R. Ramalingam[e], S. Nanthakumar[f], R. Girimurugan[g], M. Anbarasu[h] and M. Mathanbabu[i]

[a]*Dept. of Mech. Engg., Velammal Inst. Tech., Chennai, Tamil Nadu, India*
[b]*Dept. of Chemistry., Nandha Engg. College, Perundurai, Tamil Nadu, India*
[c]*Dept. of Mech. Engg., P.E.S. Inst. Tech. and Mgmt., Shivamogga, Karnataka, India*
[d]*Dept. of Electronics and Communication Engg., Koneru Lakshmaiah Education Foundation, Vaddeswaram, Andhra Pradesh, India*
[e]*Dept. of Chem. Engg., Hindusthan College of Engg and Tech., Coimbatore, Tamil Nadu, India*
[f]*Dept. of Mech. Engg., P.S.G. Inst. Tech. and Applied Research, Coimbatore, Tamil Nadu, India*
[g]*Dept. of Mech. Engg., Nandha College Tech., Perundurai, Tamil Nadu, India*
Corresponding Author, Email: mythilyvenkat2011@gmail.com
[h]*Dept. of Mech. Engg., Thanthai Periyar Govt. Inst. Tech., Vellore, Tamil Nadu, India*
[i]*Dept. of Mech. Engg., Govt. College Engg., Bargur, Krishnagiri, Tamil Nadu, India*

ABSTRACT:

This research focuses on three types of aluminium composites: AA 5052, AA5052 + SiC and AA 5052 + SiC + GSA. The composites were made by stir casting. The hardest of the hybrid composites was made from groundnut shell ash. The improvement was 75% as compared to pure AA 5052. The density was measured experimentally using the Archimedes technique and theoretically using the rules of mixture. Composition of hybrid composites were aluminum alloy 5052, aluminum alloy 5052/ silicon carbide (SiC) and aluminum alloy 5052/ SiC/ groundnut shell ash (GSA). Results were analyzed, including Material Removal Rate (MRR), Surface Roughness (SR) and Tool Wear (TW). The test results were analyzed and then optimized, using RSM. When calculating SR and MRR, feed rate was the most crucial factor. TW was shown to be most affected by tool speed, while MRR was least affected by the % wt. of reinforcement.

KEYWORDS:

Material removal rate; Hybrid composite; Feed rate; Machining parameters; Tool wear; Groundnut shell ash

CITATION:

M.S.H. Dani, N. Saravanan, L. Girisha, K.K. Uday, R. Ramalingam, S. Nanthakumar, R. Girimurugan, M. Anbarasu and M. Mathanbabu. 2024. Optimizing the properties of AA5052 alloys through Silicon Carbide and Groundnut Shell Ash Reinforcements, *Int. J. Vehicle Structures & Systems*, 16(4), 630-635. doi:10.4273/ijvss.16.4.24.

1. Introduction

AA 5052 has many applications in the mineral and chemical processing industries. Composite materials using AA 5052 chemical can have particulates and fibres added to the matrix [1]. This material largely satisfies requirements for use in automotive and aeronautical settings. Reinforcing ceramics can be made from a variety of materials, including carbonates, oxides (SiO_2, Al_2O_3) and nitrides (Si_3N_4, Al_2O_3). The AA 5052-based Metal Matrix Composites (MMCs) can be updated with these reinforcements [2, 3]. The outstanding mechanical features of MMC include tensile strength (TS), compression strength (CS) and wear resistance (WR). Composite aluminium engine blocks have mostly supplanted traditional cast iron engine blocks in modern automobiles for the benefit of reduced weight and improved fuel economy [4, 5]. There is still an issue with MMC production. MMCs are manufactured using a variety of processes, including powder metallurgy, diffusion bonding and squeeze casting [6]. Stir casting is the method of choice for manufacturing MMC because of its high efficiency and low cost. Machining processes are used to remove excess material from MMCs and to achieve the appropriate surface polish. However, MMCs are challenging to machine due to the presence of strong ceramic reinforcing [7].

Many researchers have worked to create various MMCs for various applications [8]. According to the studies, the hardness was improved by using GSA components. The AA5052 hybrid composite, which is strengthened with graphite and Al_2O_3, was developed by Girimurugan et al [9] and Priyan et al [10]. Hardness, compression strength, flexural strength and tensile strength were all demonstrated to be better in composites than in pure AA 5052. According to Patel et al [11], the AA 5052/SiC composite, which they created, has better mechanical properties than pure AA 5052. It is discovered that the hybrid composite made from AA 5052 has better mechanical properties than the AA 6061. For higher particle weight percentages, it was discovered that the hardness of a hybrid compound consisting of GSA and Gr-based Al alloy increased uniformly [12, 13]. The optimal mixture of GSA and fly ash for maximum TS and hardness was found to be 20% each [14]. It has been proven that the hardness of a composite can be improved by increasing the percentage of ceramic

phase inside it. Results and fracture strength showed that the weakest particles were the most effective in strengthening. Venkatesh et al [15] developed AA 5052/Al_2O_3 nanocomposites. When compared to unreinforced AA 6061, the mechanical properties of Al_2O_3-reinforced AA 6061 are much more favourable.

Researchers [16] created a hybrid composite out of SiC and groundnut shell ash (GSA) for use in AA 5052. Improving the surface quality of the final product while keeping production costs low by using the product's mechanical qualities is a top priority for ensuring a high-quality end result. Machineability is a barrier to commercialization for MMCs. Diamond inserts were used to fabricate silicon carbide-based aluminum alloy composites for wear study. The impact of ceramic particles on surface roughness in MMC machining is examined. Using WC carbide tools that had been coated with TiN, cut a SiC-based aluminum alloy composite [17, 33]. There was a focus on how the reinforcing particle affected the final composite's machinability. It was shown that tool wear was greatest at a high percentage of reinforcement [18]. During machining, AA 5052/SiC composite showed lower SR and TW than pure AA 5052. The surface roughness of a hybrid combination of Al_2O_3 and Gr-reinforced aluminum alloy 6061 was milled using RSM. According to the results, machining an aluminum alloy 6061/Al_2O_3/Gr hybrid compound quickly was the most important factor.

The cutting parameters for AA 5052/SiC composites were modified to improve efficiency and extend tool life [19]. Taguchi's method was used to machine polymer matrix composites and it was found [20] that as the feed rate was raised, the SR also increased. When milling AA 5052-T6, the optimal cutting settings for cutting forces. When milling AA 5052, utilized an RSM to smooth up the material's finish. It is analysed that the cutting forces and surface roughness of AA hybrid composites based on SiC. The design was optimized using the RSM method [21]. Using polycrystalline diamond cutting inserts, the SR of a turned aluminum alloy 5052/SiC composite was measured [22, 23]. A hybrid composite comprising AA 5052, SiC and GSA has recently been the subject of research into its creation and characterization. Before the material can be made available to the public, its machining properties must be thoroughly investigated.

2. Experimental work

GSA and SiC were used to reinforced with aluminium alloy 5052. After completing a ground survey to evaluate the availability and requirements, it was decided to begin with a matrix and then add reinforcements. Table 1 displays AA5052's chemical arrangement. The component was manufactured using a bottom-pouring stir casting machine. The materials used to create the final products were AA5052, AA5052 + 6% wt. SiC and AA5052 + 6% wt. SiC + 6% wt. GSA. Argon gas at a purity level of 99.99% was employed at a flow rate of 10 LPM during the casting process [24]. The melting point of graphite in a crucible is 485°C. After drying the reinforcement particles at 300°C for 40 minutes, they were combined with SiC and GSA in molten pure AA5052. The matrix and reinforcement material have a problem with wettability because of the weak contact between AA5052 and the reinforcement particles. At 415rpm, mechanical stirring was performed before the addition of SiC and GSA particles. The reinforcement particle is incorporated into the liquid AA5052 via vibrations from the reinforcement feeder attachment. Four minutes of agitation were enough to fully incorporate AA5052 with the reinforcing particles (SiC and GSA). AA5052 melt was to be poured into a die steel mould with a rectangular cavity of 20×10×250mm, as well as two cylindrical cavities measuring 25×250 and 18×250mm. For the casting process to go smoothly, it was essential to have a good vacuum in the mold before pouring in the molten metal. The temperature differential was gotten rid of by heating the mold to 450°C. The samples were removed from the mold once it had cooled. The stir casting apparatus is depicted in Fig. 1.

Table 1: Chemical composition of AA 5052

Elements	Mn	Fe	Cu	Mg	Si	Zn	Cr	Al
Wt. %	0.10	0.40	0.10	2.80	0.25	0.10	0.35	Balance

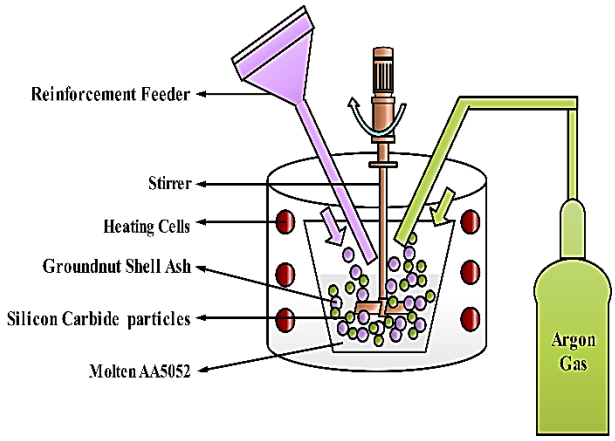

Fig. 1: Arrangement of stir casting

In this investigation, numerous turning trials were conducted using a computer numerically controlled lathe (turning machine). Machining was performed on pure AA5052, a composite of AA5052 + 6% wt. SiC and a composite of AA5052 + 6% wt. SiC + 6wt.% GSA. For the turning processes, titanium carbide inserts were used. There are eight blades on a single insert. Each operation utilized a single edge. A total of 27 tests were conducted with seven different inserts. The supplier's tool inserts are described in Table 2. All of the tests are conducted on a CNC lathe spinning dry material. All of this was done while connected to a stable power supply. The input and output data for each module are explicitly displayed. Maximizing output while lowering SR and TW is a primary focus in the manufacturing sector. The input values for the carbide inserts utilized in the machining of the workpiece were determined [25]. The input values are shown in Table 3.

Table 2: CNMG 120408 specification of plain carbide tool

Specification	Value	Specification	Value
IC size of enclosure	12.7mm	Width	4.76mm
Radius of the nose	0.8mm	Grade	TT 8125
Diameter of the hole	5.16mm	Covered angle	80°

Table 3: Input parameters and its levels

Specification	Parameter	Level		
		-1	0	+1
A	Reinforcement wt. %	0	6	12
B	Speed (m/min)	180	210	240
C	Feed (mm/rev)	0.3	0.6	0.9
D	Depth of cut (mm)	0.6	1.2	1.8

The rule of mixture was applied to estimate the theoretical density of the manufactured composite based on the matrix and reinforcing elements of the composite material using [26],

$$p_c = \rho_b \times W_b + \rho_r \times W_r + \{1 - (W_b + W_r)\} \times \rho_m \quad (1)$$

The impact resistance of the samples was measured in accordance with ASTM D256 using a Charpy/Izod pendulum tester with a 200 J capacity. The samples have a square cross section of 10×10mm. The samples' durability was determined using a Mitutoyo HM 100 series Vicker's hardness tester. In accordance with ASTM E-384, we applied stress at a rate of 5 N for 15 seconds [27]. The average of the three measured hardness was determined.

3. Results and discussions

More peaks and troughs mean a higher SR value and vice versa. Mitutoyo SJ-301 contact SR tester was used to get the reading. The surface roughness was evaluated using an 800mm threshold. Three separate measurements were taken on the Ra of machined tasters and the average was used. MRR is calculated as [28],

$$MRR = ((Wbm - Wam))/T \quad (2)$$

Whereas, W_{bm} = initial weightage machining (gms), W_{am} = final weightage machining (gms) and T = turning time (seconds). Adding tough SiC particles to AA 5052 increased the material's resistance to impact. The observed boost can be attributed to the amplification of plastic deformation energy. When AA5052/SiC and 5052/SiC/GSA is utilized, the materials have a greater fracture energy requirement. The reinforcement's impact strength effect is shown in Fig. 2. Several samples of compounds were tested for hardness and the results are shown in Fig. 3. It was shown that by including SiC and GSA, the hardness will increase.

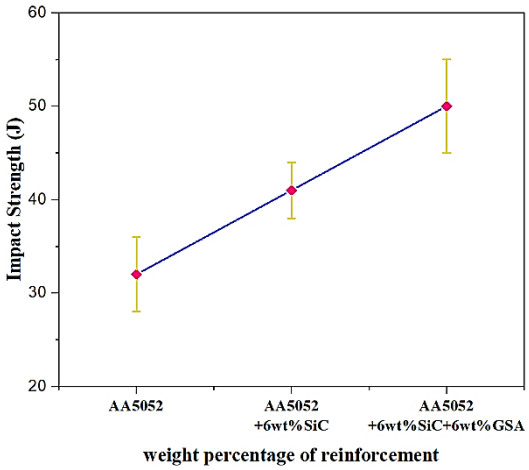

Fig. 2: Effect of reinforcement on the impact strength

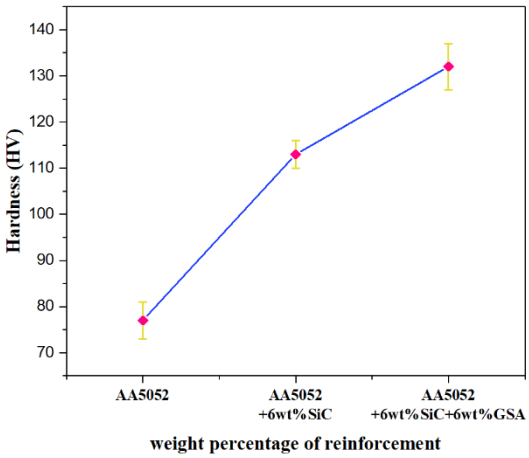

Fig. 3: Effect of reinforcement on the hardness

Particles composed with AA5052, SiC and GSA are less dense than pure AA5052. The results, displayed in Fig. 4, reveal that the composite's theoretical density was slightly lower than its measured value. GSA has a lower particle density than SiC and a higher matrix density than AA5052. Because of the presence of groundnut shell ash particles, the final composite has a lower density [29]. In order to determine if a material can be machined, researchers use CNC lathe machines in lab settings. The SR, TW and MRR were calculated. Each trial's results were analyzed thrice. In this work, we provide an average of the responses obtained. The outcomes of the tests are tabulated in Table 4.

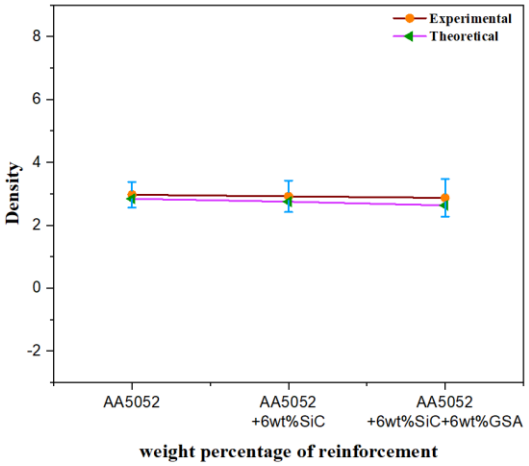

Fig. 4: Effect of reinforcement on the density

Table 4: Experimental result

A %	B (m/min)	C (mm/rev)	D (mm)	MRR (g/min)	SR (µm)	TW (µm)	Std. order units	Run order
6	270	0.6	1.2	11.8	1.22	74.8	20	1
12	180	0.9	0.6	18.3	0.99	70.3	6	2
12	180	0.3	1.8	13.8	1.73	75.9	10	3
6	210	0.6	2.4	19.8	1.53	45.3	24	4
6	150	0.6	1.2	13.3	1.12	33.8	19	5
6	210	1.2	1.2	16.3	1.59	76.3	22	6
6	210	0.6	1.2	11.8	1.25	105.1	25	7
0	180	0.9	0.6	12.8	1.43	50.3	5	8
-6	210	0.6	1.2	15.3	1.24	56.8	17	9
0	240	0.9	1.8	18.8	1.61	44.9	15	10
18	210	0.6	1.2	18.8	0.97	33.1	18	11

0	180	0.3	0.6	10.8	0.99	57.5	1	12
12	180	0.9	1.8	22.3	0.77	25.3	14	13
6	210	0.6	1.2	12.3	1.68	80.3	27	14
6	210	0.6	1.2	23.8	1.04	55.1	26	15
6	210	0.6	0	22.8	1.28	56.5	23	16
12	240	0.3	1.8	13.3	1.33	50.6	12	17
0	180	0.9	1.8	14.8	1.4	69.2	13	18
0	240	0.9	0.6	14.3	1.39	37.1	7	19
0	180	0.3	1.8	10.3	1.28	57.3	9	20
6	210	0	1.2	20.3	1.07	34.1	21	21
12	180	0.3	0.6	14.3	0.93	35.3	2	22
12	240	0.9	1.8	11.3	1.24	36.86	16	23
0	240	0.3	1.8	18.8	0.87	74.88	11	24
0	240	0.3	0.6	14.8	0.96	35.3	3	25
12	240	0.9	0.6	16.8	0.86	33.3	8	26
12	240	0.3	0.6	8.3	1.63	80.94	4	27

To study the roughness of the surface, we employed a modified cubic model. To reduce complexity, we employ a power transformation, where y' = (y+k), =0.95 and k = 0. We used the values of k and λ to get a good fit for the data. The selected model's significance was verified by ANOVA. The results of an ANOVA on the connection between roughness and surface quality are shown in Table 5. A modified cubic model is utilized to mimic tool wear and tear. An inverse square root transformation was used to simplify the form y' = 1 / Square root (y+k), where k = 2.5, which improved the model's applicability [30]. To ensure the model was adequate, ANOVA was used.

Table 5: ANOVA for SR

Source	Sum of squares	Df	Mean square	F-value	p-value
Model	1.21	14	0.0867	1.35	0.3027
Reinf. % wt.	0.0408	1	0.0408	0.6375	0.4401
B-Speed	0.0135	1	0.0135	0.2113	0.6540
C-Feed	0.0425	1	0.0425	0.6635	0.4312
D-Depth of cut	0.1001	1	0.1001	1.56	0.2351
AB	0.0518	1	0.0518	0.8079	0.3864
AC	0.7613	1	0.7613	11.88	0.0048
AD	0.0046	1	0.0046	0.0711	0.7942
BC	0.0264	1	0.0264	0.4122	0.5329
BD	0.0248	1	0.0248	0.3872	0.5454
CD	0.0077	1	0.0077	0.1195	0.7356
A^2	0.0798	1	0.0798	1.25	0.2863
B^2	0.0430	1	0.0430	0.6712	0.4286
C^2	0.0005	1	0.0005	0.0080	0.9303
D^2	0.0041	1	0.0041	0.0639	0.8047
Residual	0.7688	12	0.0641		
Lack of fit	0.5559	10	0.0556	0.5223	0.8023
Pure error	0.2129	2	0.1064		
Cor. total	1.98	26			

The outcomes of TW model's ANOVA are shown in Table 6. Without making any other adjustments, the data were fitted using the quadratic model. Table 7 shows that the chosen model was supported by ANOVA table for the MRR. The cutting speed, cutting depth, feed and reinforcing wt. % are the most important factors. TW was shown to be largely affected by two variables: cutting depth and feed rate. Maximizing the feed rate and cut depth helps with this issue. The research shows that lowering speed matters more than anything else when figuring out TW. As cutting speed increases, tool wear also increases. The friction between tool and workpiece causes heat to build up quickly. Heat generated at the tooltip increases the rate of thermostability in the material and wear [31]. Fig. 5 shows TW procedure. There are two distinct processes that begin once a carbide tool contacts a spinning piece of aluminium alloy 5052. AA5052/SiC composite wears faster when the tip makes contact. The increased wear seen in Case 2 is the result of hard SiC particles contacting the tool tip. The hybrid composite of AA5052/SiC/GSA decreased tool wear. The GSA reinforcement greatly enhanced the material's machinability [32]. The main objective of optimization is to either maximize or eliminate some quantity. SR, TW and MRR are the outcomes measured in this investigation.

Table 6: ANOVA for TW

Source	Sum of squares	df	Mean square	F-value	p-value
Model	4009.32	14	286.38	0.5432	0.8623
Reinf. wt. %	178.11	1	178.11	0.3378	0.5718
B-speed	50.40	1	50.40	0.0956	0.7625
C-feed	10.75	1	10.75	0.0204	0.8888
D-depth of cut	6.51	1	6.51	0.0123	0.9134
AB	85.66	1	85.66	0.1625	0.6940
AC	178.89	1	178.89	0.3393	0.5710
AD	591.22	1	591.22	1.12	0.3105
BC	386.71	1	386.71	0.7335	0.4085
BD	2.48	1	2.48	0.0047	0.9464
CD	259.05	1	259.05	0.4914	0.4967
A^2	1600.91	1	1600.91	3.04	0.1069
B^2	853.51	1	853.51	1.62	0.2273
C^2	793.87	1	793.87	1.51	0.2433
D^2	1098.32	1	1098.32	2.08	0.1745
Residual	6326.17	12	527.18		
Lack of fit	5076.15	10	507.61	0.8122	0.6674
Pure error	1250.03	2	625.01		
Cor. Total	10335.50	26			

Table 7: ANOVA for MRR

Source	Sum of squares	df	Mean square	F-value	p-value
Model	209.60	14	14.97	0.8053	0.6542
Reinf. wt. %.	4.17	1	4.17	0.2241	0.6444
B-speed	0.6667	1	0.6667	0.0359	0.8530
C-feed	12.04	1	12.04	0.6477	0.4366
D-depth of cut	2.04	1	2.04	0.1098	0.7461
AB	85.56	1	85.56	4.60	0.0531
AC	10.56	1	10.56	0.5682	0.4655
AD	3.06	1	3.06	0.1647	0.6920
BC	10.56	1	10.56	0.5682	0.4655
BD	0.5625	1	0.5625	0.0303	0.8648
CD	0.5625	1	0.5625	0.0303	0.8648
A^2	0.6690	1	0.6690	0.0360	0.8527
B^2	36.17	1	36.17	1.95	0.1883
C^2	0.3912	1	0.3912	0.0210	0.8871
D^2	16.72	1	16.72	0.8996	0.3616
Residual	223.08	12	18.59		
Lack of fit	130.92	10	13.09	0.2841	0.9304
Pure error	92.17	2	46.08		
Cor. total	432.69	26			

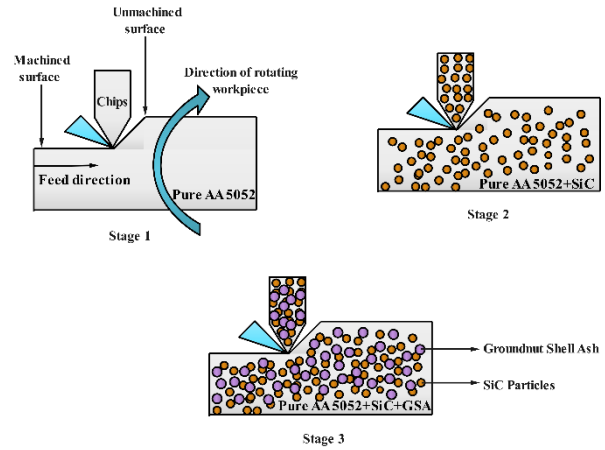

Fig. 5: Tool wear mechanism of AA5052, AA5052/SiC composite and AA5052/SiC/GSA hybrid composite

Multi-response optimization considers all possible replies, allowing for the simultaneous optimization of all input parameters. This is enhanced by employing a desirability analysis. The optimization goals and allowed parameter space are detailed in Table 8. Fig. 6 displays that the optimal settings for this operation were 1.61691% reinforcement, 0.814347 mm/rev feed rate, 210.662 m/min cutting speed and 1.8 mm depth of cut. We obtained an MRR of 17.1059 g/min, an SR of 1.51209 m and a TW of 70.521m by setting the parameters to these values.

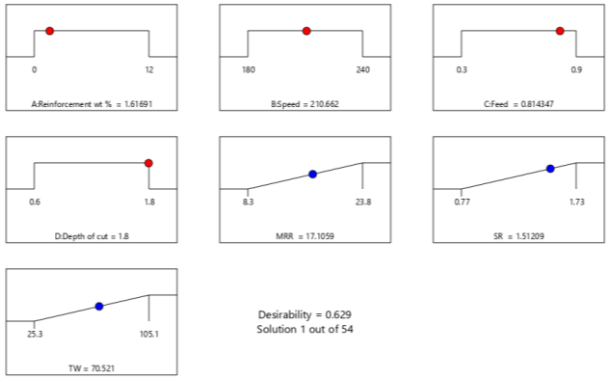

Fig. 6: Desirability ramp graph

Table 8: Optimization goal and input levels

Inputs	Goal	Min. limit	Max. limit	Significance
A	In limit	0	12	10
B	In limit	180	240	5
C	In limit	0.3	0.9	5
D	In limit	0.6	1.8	5
MRR	Minimum	8.3	23.8	5
SR	Minimum	0.77	1.73	5
TW	Minimum	25.3	105.1	5

4. Conclusion

The AA5052-SiC-GSA hybrid compound was successfully produced using the stir casting method. The hybrid composite's mechanical and machining qualities were rated based on its hardness. These results are based on the experimented and RSM optimization. The strength increases in proportion to the percentage of reinforcement in the total weight. The hardest material was an AA5052 + 6% SiC + 6% GSA composite. The purity of AA5052 is 75% higher. Because of this, the hardness of AA5052 has been increased by including a ceramic phase. Feed rate has a major impact on both MRR and surface roughness. % wt. of reinforcement is regarded to have relatively little impact on TW, while speed is the most critical factor in determining MRR. A speed of 210.662 m/min, a feed rate of 0.814347 mm/rev and a depth of cut of 1.8 mm were found to be optimal.

REFERENCES:

[1] J. Sarvaiya and D. Singh. 2022. Influence of hybrid pin profile on enhancing microstructure and mechanical properties of AA5052/SiC surface composites fabricated via friction stir processing, *Canadian Metallurgical Quarterly*, 62(3), 426-439. https://doi.org/10.1080/00084433.2022.2114124.

[2] M. Faraji, S. Karimi, M. Esmailzadeh, L. Pezzato, I. Calliari and H. Eskandari. 2022. The electrochemical and microstructure effects of TiB_2 and SiC addition to AA5052/Al_2O_3 surface composite coatings in 0.5 M H_2SO_4 solution, *J. Bio-& Tribo-Corrosion*, 8, 117. https://doi.org/10.1007/s40735-022-00716-7.

[3] R. Girimurugan, N. Senniangiri, B.P. Krishnan, S. Kavitha and M. Vairavel. 2021. Tensile behaviour of hybrid polymer composites - An experimental study, *IOP Conf. Series: Mat. Sci. & Engg.*, 1059. https://doi.org/10.1088/1757-899X/1059/1/012033.

[4] M. Faraji, S. Karimi, M. Esmailzadeh and L. Pezzato. 2023. Investigation of the microstructure and corrosion behaviors of composite hard-faced layers on Al5052 using SiC and TiB_2 in 3.5% NaCl and 0.5 M H_2SO_4 solutions, *J. Mat. Engg. & Performance*, 32, 9711-9724. https://doi.org/10.1007/s11665-023-07807-7.

[5] M. Patel, S.K. Sahu and M.K. Singh. 2020. Abrasive wear behavior of SiC particulate reinforced AA5052 metal matrix composite, *Mat. Today: Proc.*, 33(8), 5586-5591. https://doi.org/10.1016/j.matpr.2020.03.572.

[6] D.D. Kumar, A. Balamurugan, K.C. Suresh, R.S. Kumar, N. Jayanthi, T. Ramakrishnan, S.K.H. Ahammad, S. Mayakannan and S.V. Prabhu. 2023. Study of microstructure and wear resistance of AA5052/B_4C nanocomposites as a function of volume fraction reinforcement to particle size ratio by ANN, *J. Chem.*, 2023(1), 1-12. https://doi.org/10.1155/2023/2554098.

[7] N. Selvakumar, M.J.S. Mohamed, R. Narayanasamy and K. Venkateswarlu. 2013. Forming limit diagram and void coalescence analysis of AA5052 coated with molybdenum-based ceramic nanocomposites, *Mat. & Design*, 52, 393-403. https://doi.org/10.1016/j.matdes.2013.05.052.

[8] S. Kim, J. Hong, Y. Joo and M. Kang. 2022. Synergistic effect of SiC nano-reinforcement and vibrator assistance in micro-friction stir welding of dissimilar AA5052-H32/AA6061-T6, *J. Mfg. Processes*, 82, 860-869. https://doi.org/10.1016/j.jmapro.2022.08.023.

[9] R. Girimurugan, R. Pugazhenthi, T. Suresh, P. Maheskumar and M. Vairavel. 2021. Prediction of mechanical properties of hybrid aluminium composites, *Mat. Today: Proc.*, 39(1), 712-716. https://doi.org/10.1016/j.matpr.2020.09.302.

[10] V.G.S. Priyan, R. Malayalamurthi and S.K. Subbu. 2020. Investigation on wear behaviour of AA5052/SiC/Al_2O_3 hybrid composite fabricated using stir casting process,

Adv. Applied Mech. Engg., 975-982. https://doi.org/10.1007/978-981-15-1201-8_104.

[11] M. Patel and S.K. Sahu. 2023. Effect of SiC particulate content on the abrasive wear parameters of AA5052 matrix, *Recent Adv. Mech. Engg.*, 577-587. https://doi.org/10.1007/978-981-99-2349-6_52.

[12] M. Bodaghi and K. Dehghani. 2017. Friction stir welding of AA5052: The effects of SiC nano-particles addition, *Int. J. Adv. Mfg. Tech*., 88, 2651-2660. https://doi.org/10.1007/s00170-016-8959-8.

[13] M. Vairavel, R. Pughazhenthi, R. Girimurugan, S. Vinothkumar and N. Poornachandiran. 2020. Effects of wear characterization analysis of the friction stir welded joints in aluminum alloy Al3116-Cu and A384-Cu, *AIP Conf. Proc*., 2283(1), 020112. https://doi.org/10.1063/5.0025005.

[14] C.M. Ikumapayi, C. Arum and K.K. Alaneme. 2021. Reactivity and hydration behavior in groundnut shell ash based pozzolanic concrete, *Mat. Today: Proc*., 38(2), 508-513. https://doi.org/10.1016/j.matpr.2020.02.385.

[15] L. Venkatesh, T.V Arjunan, M. Arulraj and K. Ravikumar. 2022. Study on tribological behaviour of aluminium hybrid composites strengthened with novel groundnut shell ash and boron carbide, *Proc. Inst. Mech. Engg., Part E J. Process Mech. Engg*., 237(2), 350-363. https://doi.org/10.1177/09544089221112162.

[16] S. Vinoth, C. Rajasekar, P. Sathish, V. Sureshkumar, A. Yasminebegum, S.H. Ahammad and R. Girimurugan. 2023. Optimization of process parameters on wire cut electrical discharge machining and surface integrity studies of AA6070/MgO composites, *Proc. Int. Conf. Mat. Sci., Mechanics & Tech*., Indore, India. https://doi.org/10.1088/1742-6596/2484/1/012012.

[17] K.K. Alaneme, M.O. Bodunrin and A.A. Awe. 2018. Microstructure, mechanical and fracture properties of groundnut shell ash and silicon carbide dispersion strengthened aluminium matrix composites, *J. King Saud Univ. -Engg. Sci*., 30(1), 96-103. https://doi.org/10.1016/j.jksues.2016.01.001.

[18] L. Venkatesh, T.V. Arjunan and K. Ravikumar. 2019. Microstructural characteristics and mechanical behaviour of aluminium hybrid composites reinforced with groundnut shell ash and B_4C, *J. Brazilian Society Mech. Sci. & Engg.*, 41, 295. https://doi.org/10.1007/s40430-019-1800-1.

[19] R. Manikandan, P. Ponnusamy, S. Nanthakumar, A. Gowrishankar, V. Balambica, R. Girimurugan and S. Mayakannan. 2023. Optimization and experimental investigation on AA6082/WC metal matrix composites by abrasive flow machining process, *Mat. Today: Proc*., 1-5. https://doi.org/10.1016/j.matpr.2023.03.274.

[20] R. Butola, A. Malhotra, M. Yadav, R. Singari, Q. Murtaza and P. Chandra. 2019. Experimental studies on mechanical properties of metal matrix composites reinforced with natural fibres ashes, *SAE Tech. Paper*, 1-11. https://doi.org/10.4271/2019-01-1123.

[21] R. Butola, V. Sharma, S. Kanwar, L. Tyagi, R.M. Singari and M. Tyagi. 2020. Optimizing the machining variables in CNC turning of aluminum based hybrid metal matrix composites, *SN Applied Sci*., 2, 1356. https://doi.org/10.1007/s42452-020-3155-8.

[22] S.P. Dwivedi, M. Maurya, N.K. Maurya, A.K. Srivastava, S. Sharma and A. Saxena. 2020. Utilization of groundnut shell as reinforcement in development of aluminum based composite to reduce environment pollution: A review, *Evergreen*, 7(1), 15-25. https://doi.org/10.5109/2740937.

[23] B. Babu, S. Meinathan, P. Manikandan, P. Lingeswaran, S. Nanthakumar, A. Yasminebegum and R. Girimurugan. 2023. Investigation on the characterization of hot extruded AA7075 based metal matrix composites developed by powder metallurgy, *Proc. National Conf. Physics & Chem. Mat.*, Indore, India. https://doi.org/10.1088/1742-6596/2603/1/012041.

[24] S. Jadhav, A. Aradhye, S. Kulkarni, Y. Shinde and V. Vaishampayan. 2019. Effect of hybrid ash reinforcement on microstructure of A356 alloy matrix composite, *AIP Conf. Proc*., 020010. https://doi.org/10.1063/1.5100695.

[25] A.S. Kanthasamy, T.S. Ravikumar, S. Anish, V. Hariram, S.R.K. Lindsay, D.G. Adarsh, S. Anirudh, V.B. Ankireddy and P.I. Khan. 2023. Influence of groundnut shell ash particle (GSAp) addition on mechanical and corrosion behaviour of AZ31 magnesium alloy, *Int. J. Vehicle Structures & System*, 15(1), 101-104. https://doi.org/10.4273/ijvss.15.1.19.

[26] M. Palanivendhan and J. Chandradass. 2021. Experimental investigation on mechanical and wear behavior of agro waste ash-based metal matrix composite, *Mat. Today: Proc.*, 45(7), 6580-6589. https://doi.org/10.1016/j.matpr.2020.11.712.

[27] A. Verma, A. Pal, S.P. Dwivedi and S. Sharma. 2019. Physical, mechanical and thermal behavior of recycled agro waste GSA reinforced green composites, *Mat. Testing*, 61(9), 894-900. https://doi.org/10.3139/120.111399.

[28] V.K. Krishnan, J.V. John and R. Girimurugan. 2023. Optimization of drilling parameters in vertical machining centre drilling on magnesium AZ91D alloy under dry condition with Taguchi design, *Mat. Today: Proc*., online. https://doi.org/10.1016/j.matpr.2023.08.121.

[29] J.C. Galvis, P.H.F. Oliveira, M.F. Hupalo, J.P. Martins and A.L.M. Carvalho. 2017. Influence of friction surfacing process parameters to deposit AA6351-T6 over AA5052-H32 using conventional milling machine, *J. Mat. Processing Tech*., 245, 91-105. https://doi.org/10.1016/j.jmatprotec.2017.02.016.

[30] M. Gopinath and N. Senthilkumar. 2023. Improving productivity through maximizing MRR in machining silicon nitride ceramic reinforced aluminium alloy 5052, *Mat. Today Proc*., 79(1), 122-126. https://doi.org/10.1016/j.matpr.2022.09.542.

[31] L.N. Katta, M. Natarajan, T. Pasupuleti, P. Sivaiah and S.C.N. Venkata. 2022. Neural network model for machinability investigations on CNC turning of AA5052 for marine applications with MQL, *SAE Technical Paper*, 1-6. https://doi.org/10.4271/2022-28-0515.

[32] V. Edachery, S. Ravi, A.F. Badiuddin, A. Tomy, S.V. Kailas and P.S. Suvin. 2022. Wetting behaviour of a green cutting fluid (GCF); influence of surface roughness and surface energy of AA5052, Ti6Al4V and EN31, *Mat. Today Proc.*, 62(14), 7605-7609. https://doi.org/10.1016/j.matpr.2022.04.835.

[33] S.R. Rallabandi, L. Srinivas, S. Palli, R.C. Sharma, N. Sharma, A. Sharma and S.K. Sharma. 2024. A contrastive characterization of pure Mg and AZ91D alloy based on the testing of mechanical, corrosion, wear, and erosion properties, *Engineering Research Express*, 6(1), 015017. https://doi.org/10.1088/2631-8695/ad16a2.